New possibilities for damage prediction from tunnel subsidence using aerial LiDAR data

D.F. Laefer, T. Hinks
University College Dublin, Ireland

H. Carr
University of Leeds, United Kingdom

ABSTRACT: Computation modelling has not been fully exploited for predicting building damage due to tunnel-induced subsidence, because of the expense and time required to create computational meshes for the vast quantity of buildings that may be impacted along a tunnel's route. A possible circumvention of such a resource commitment lies in the exploitation of remote sensing data in the form of aerial laser scans (also know as Light Detection and Ranging – LiDAR). This paper presents work accomplished to date in the creation of a pipeline to automate the conversion of aerial LiDAR point cloud data directly into Finite Element Method (FEM) meshes without the intermediary step of triangulation-based conversion or reliance on geometric primitives through a Computer Aided Design (CAD) program. The paper highlights recent advances in flight path planning, data processing, plane identification, wall segmentation, and data transformation.

1. INTRODUCTION

Given increasing pressures of urbanization, population growth, and heightened concerns about sustainability and environmental impacts, the importance of tunnels in providing transportation options and basic utilities continues to grow. Yet, the complexity of constructing such infrastructure beneath cities has also expanded because of the myriad of existing subsurface installations and the density of aboveground structures, which need protecting from potential subsidence problems.

Yet, despite these risks and the large quantities of funding regularly committed to building monitoring during tunnelling and the requirement to pay for post-construction damage, the most advanced computational tools, such as FEM meshing, are rarely applied to the vast majority of structures that are subjected to tunnel-induced ground movements; because the cost of surveying the structures and then generating the meshes is prohibitive.

Much of the expense is related to the collection of geometrically accurate data for the structures themselves and their proximity to the tunnel. For the vast majority of existing structures no measured drawings (either design or as-built) exist, to say nothing of electronic CAD models that could easily be prepared as input files for FEM programs. Instead, a team of surveyors must be sent out to each building to measure and record all critical dimensions. This information must then be converted into a format appropriate for solid modelling. The expense of this is typically two weeks of full-time work. Thus, to do this for each of the hundreds (if not thousands) of structures along a tunnel route is simply cost prohibitive. To circumvent this, an alternative approach is proposed.

2. BACKGROUND

In 2006, the authors began developing a pipeline to auto-generate FEM meshes from a form of remote sensing data referred to as laser scanning or Light Detection and Ranging (LiDAR); as extensive information about LiDAR is readily available elsewhere, it is not included herein (e.g. Baltsavias, 1999).

The goal of the research program was to overcome the expense of present manual meshing approaches by processing the remote sensing data in a way that enabled further computational manipulation. This work plan vastly differs from the context in which virtual cities are generated, as the goal was not to create visually compelling images but ones that were spatially accurate and capable of being automatically transformed into solid models compatible for FEM processing. The work presented herein represents progress to date on this ambitious undertaking.

3. METHODOLOGY

An effective pipeline for auto-generation of FEM models from LiDAR data requires several major steps: (1) adequate data capture; (2) accurate data positioning; (3) wall identification; (4) three-dimensional building component determination; (5) data transformation; and (6) optimization.

(1) Adequate data capture

Traditionally aerial LiDAR has been used to generate digital elevation models (DEMs) or digital terrain models (DTMs). Often the purpose was for flood-plain mapping (Hollaus et al., 2005). Although there are examples of further processing to determine maximum building heights and tree growth elevation (e.g. Laefer & Pradhan, 2006), there has been relatively little emphasis on façade detail capture. However, for building damage prediction good façade information is critical, especially with respect to identifying window openings, as this strongly influences a building's stiffness (Truong-Hong & Laefer, 2010).

Because the previous emphasis of LiDAR was on horizontal elevation capture, a new paradigm was needed to maximize the vertical data capture and overcome urban shadowing problems (as described at length in Hinks et al. 2009a). The solution involved a triple overlap of the flight path (Fig. 1) oriented 45 degrees rom general city grid orientation (Fig. 2), as shown for the Dublin city-centre study area. The results are significantly better than what has traditionally been captured. In Fig. 3a density is approximately 35 points/m^2 on the f ground, while in Fig. 3b it is around 225 points/m^2.

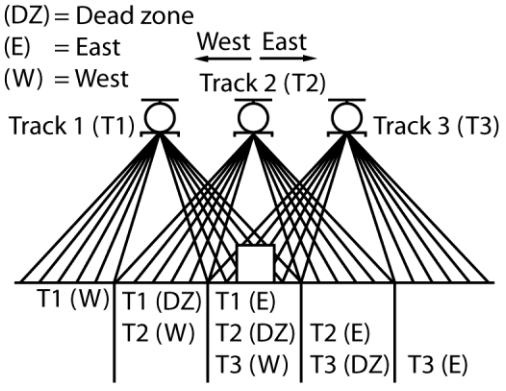

Figure 1. Triple overlap flight path needed to capture roof features and façade details.

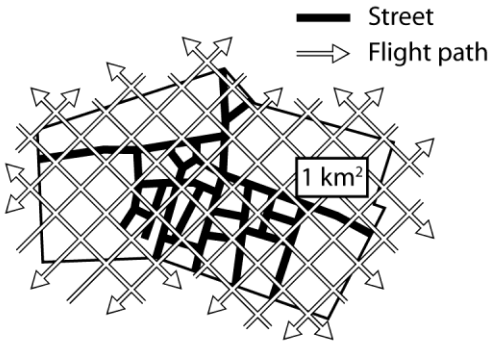

Figure 2. Flight orientation set 45 degrees from general street layout over the Dublin, Ireland city-centre study area.

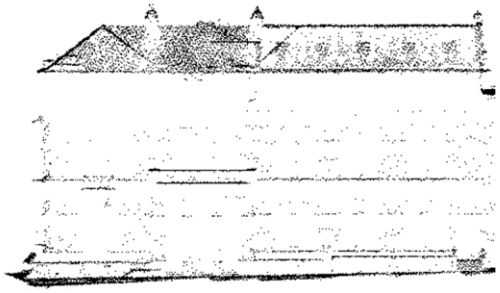

(a) LiDAR from a conventional, single path flyover

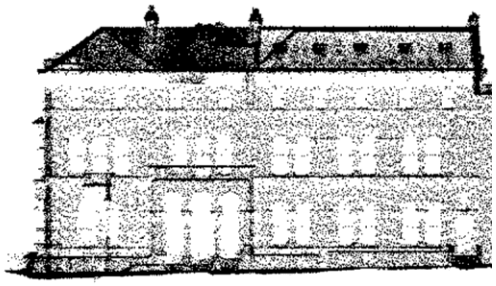

(b) LiDAR from a multi-path swath flyover

Figure 3. Traditional single pass resolution shown in (a) and multi-path results displayed in (b).

This flyover generating approximately 700 million data points was done in February 2007 at altitudes ranging from 350m to 400m. By surface modelling the data, a rapid visual comparison can be made with the terrestrial equivalent, which required 30 times the cost and nearly 1,000 times the duration (per building) to achieve the improved results (Fig. 4). Since that time, new aerial hardware has been released, with the potential of doubling the density depicted in Fig. 4. So although the aerial data is not yet equivalent in quality to the terrestrial

scans, its potential is now clear, and most likely, it is simply a matter of time for the technology to generate a financially and temporally viable output.

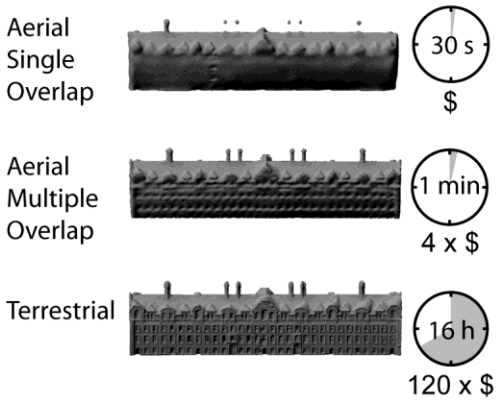

Figure 4. Surface rendering of three approaches to LiDAR data capture.

In terms of achieving computational models from this data relevant to the tunnelling community, a critical aspect is accurate window detection as apertures strongly influence in-plane wall stiffness.

(2) Accurate data positioning

To generate spatially correct urban-scale models, the data must be properly represented in their actual locations. Inherent to this is developing and understanding the data capture mechanism's role in further data processing. The integral parts of a LiDAR flight path involve multiple flight tracks, and within each are flight track segments (Fig. 5). Each flight track segment is composed of multiple scan lines. Each scan line has multiple pulses, each of which may or may not have multiple returns depending upon the reflectivity and opacity of the material (Fig. 5). Each return generates a data point with an x-, y-, and z-positional locator based on simultaneous collection of global positioning system (GPS) data. The data may also have a co-registered set of red, green, and blue (RGB) colour values. There is an inherent relationship between the scanner and the point of data capture. Understanding this relationship allows previously ignored latent data to be used as part of the post-processing procedures. Details of the development of specific geometric relationships are described elsewhere (Hinks et al. 2009a and b).

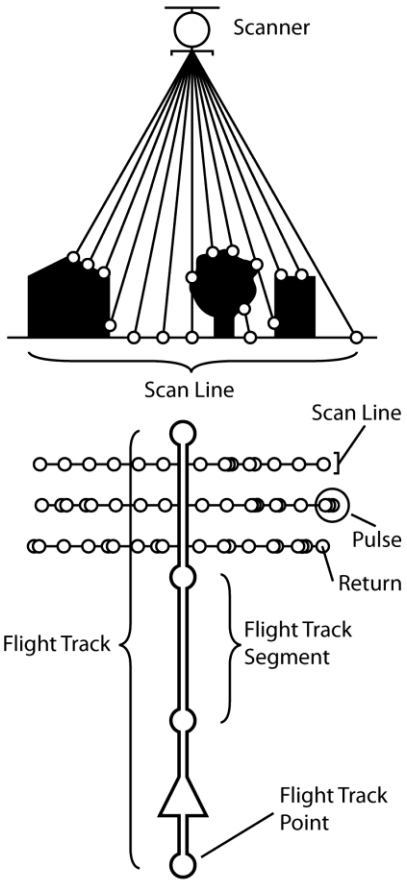

Figure 5. Component elements of LiDAR data capture.

Knowing the true location of a point allows it to be clustered with other points. Then, the point density can be used as a key indicator of the underlying three-dimensional (3D) geometry of an environment. As an example, in Fig. 6a, the data has been processed using a single value maximum height field. In contrast, Fig. 6b applies pixel intensities proportional to visibility. The visual results are of a significantly higher quality and are of a clarity level that they could be mistaken for an aerial photograph.

(3) Wall identification

A common method for wall identification relies upon a single height field criterion or other methods that require some a priori knowledge of the specific built environment (Rottensteiner, 2003, Forlani et al. 2006). Fig. 7a shows the data processed based upon the maximum elevation. The approach poses the significant

challenge of selecting a single value over which the data is classified as belonging to a building and below which is categorized as not a building (e.g. trees, buses, signage, street furniture, etc.).

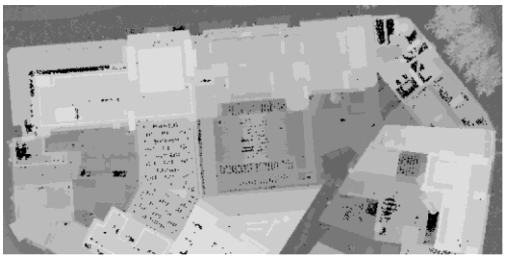

(a) Traditional, vertical data projection using single value of maximum height field to define visual representation.

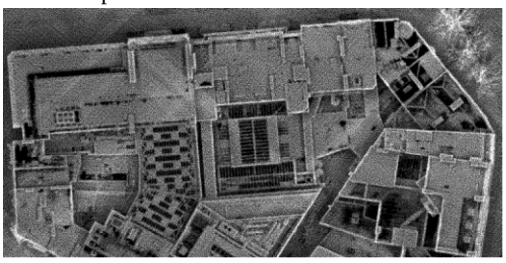

(b) New, visibility projection used to define pixel intensities.

Figure 6. Comparative visualization approaches.

When a low threshold value is used, tree and other data related to tall objects that are not buildings are unintentionally included (Fig. 7b). As the threshold value increases, the percentage of trees and similar objects decreases, but single storey buildings are then erroneously omitted (Fig. 7c). By selecting a sufficiently high threshold to avoid all foliage, significant loss of potential structures occurs (Fig. 7d). In short the approach fails except in environments of nearly uniform building elevations, where the height of non-building items is clearly distinctive from building heights. In Dublin, the dual presence double-decker buses and Georgian townhouses of similar scale makes this an especially challenging approach to adopt.

As an alternative first step for identifying the locations of buildings, the geometric relationships and the latent flight path data can be used to determine the exact locations of missing data (Fig. 8) that is a function of when a pulse encounters glass or another highly reflective material and no return is generated. As buildings are in part comprised of windows, the quantity of vertical façade data that is captured is then necessarily reduced.

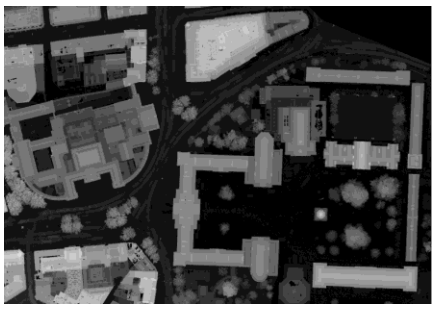

(a) Single elevation depiction.

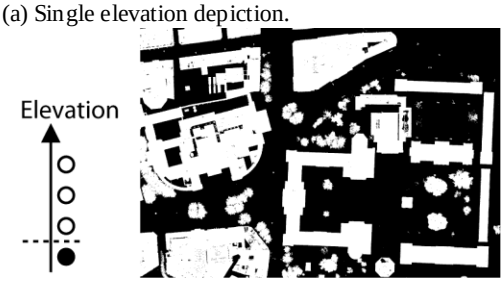

(b) Low elevation threshold criterion.

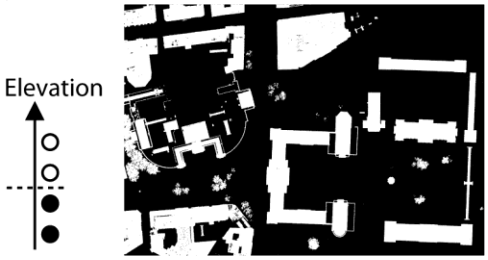

(c) Medium elevation threshold criterion.

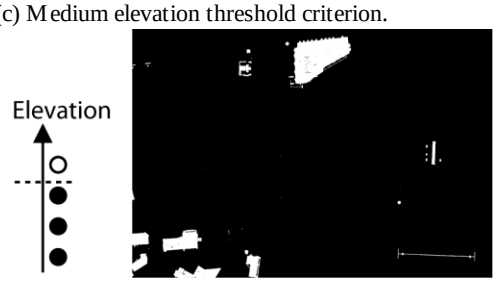

(d) High elevation threshold criterion.

Figure 7. Application of a single elevation threshold for building detection.

To help find the specific walls for a structure, this missing information can be identified and temporarily placed into the data set (Fig. 8).

(4) Three-dimensional building component determination

The fourth step is to identify data from specific walls so that they can be grouped. Each wall must be identified, and then each of the walls

must be affiliated with each other and the relevant roof structure (Fig. 9).

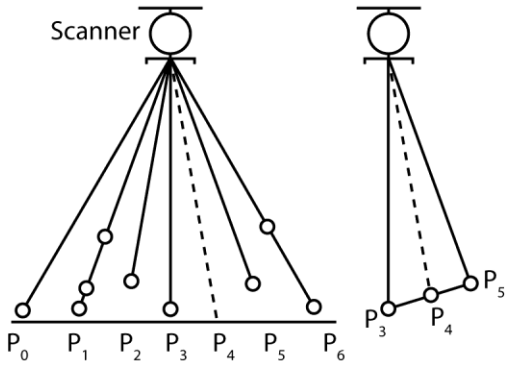

Figure 8. Temporary insertion of missing pulse, P_4.

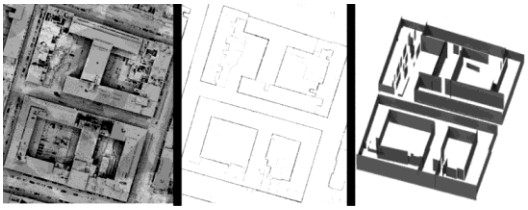

Figure 9. Preliminary wall identification. Left: LiDAR data; Middle: Wall outlines; Right: Wall generation.

The traditional workflow is shown in Fig. 10(left) where the data is vertically projected into various bins and then processed based on the single elevation criterion. Fig. 10(right), instead, schematically represents the newly proposed workflow in which angular binning occurs, and a statistically based processing is applied through contour analysis to connect the walls to each other.

The edges of individual buildings can be discerned (Fig. 11) by coupling statistical analysis with the known location of the scanner (to help determine what openings are interior courtyards) and a set of contour analysis based rules (Fig. 12). The successful identification of an actual building is verified by flood-filling the area between connected walls (Fig. 13). The results of traditional processing (Fig. 14a) are shown for the entire study area, in comparison to what is now achievable (Fig. 14b).

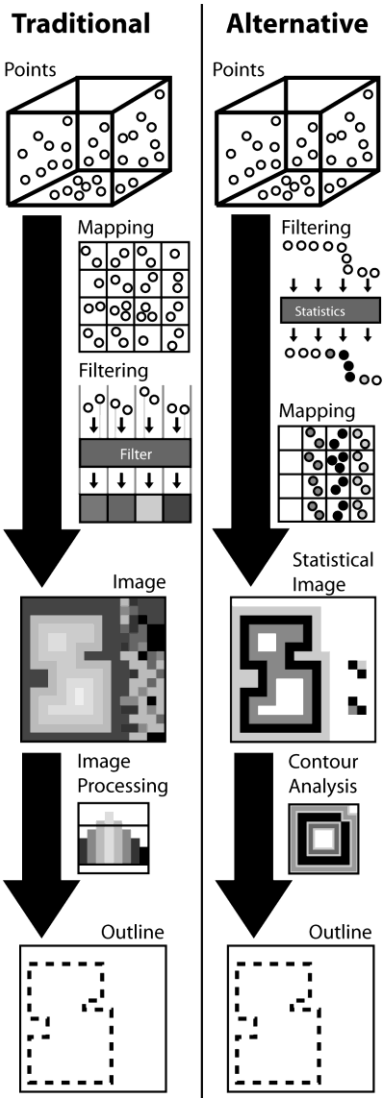

Fig. 10. Outline wall detection workflow.

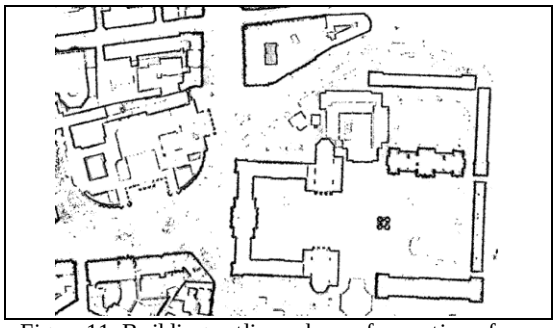

Figure 11. Building outlines shown for portion of study area.

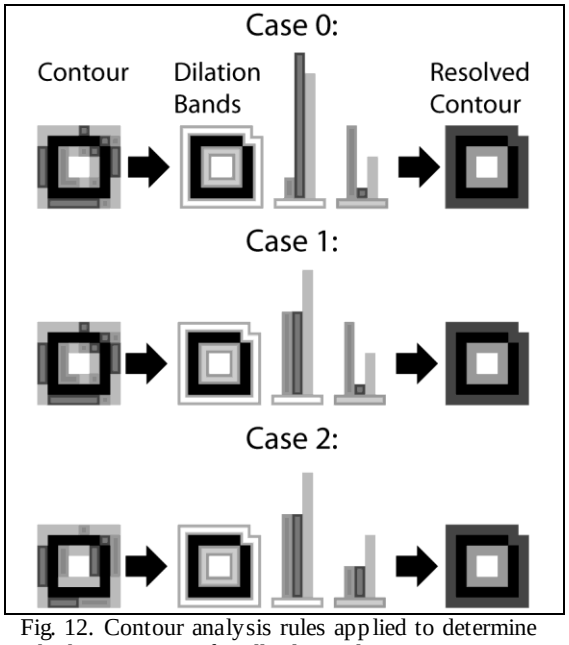

Fig. 12. Contour analysis rules applied to determine whether a group of walls do or do not represent a building.

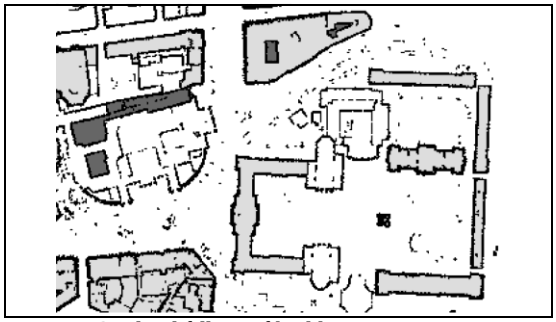
Figure 13. Flood filling of building contours as a means of verification of individual building identification.

Although not foolproof, automated building detection is vastly improved (Fig. 14a versus Fig. 14b). In some cases structures are still not visible, but the majority of buildings are identified (Fig. 14b). Of note is that this improved performance has been achieved without any a priori knowledge of the buildings, their floor plans, or the street locations. Also, the method is robust in the sense that it does not detect any false positives.

(5) Data Transformation

Once a building has been identified, the data affiliated with it can be segregated for further processing. As this step is still in progress, groups of data have been manually selected and removed for the next step in pipeline development.

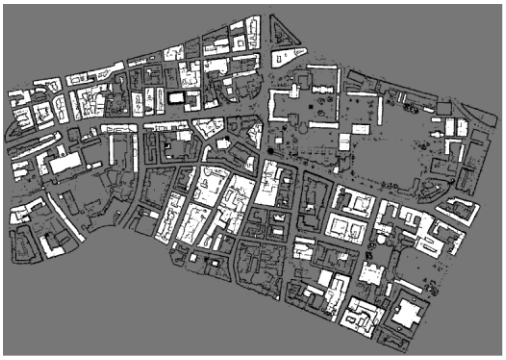
(a) Traditional processing.

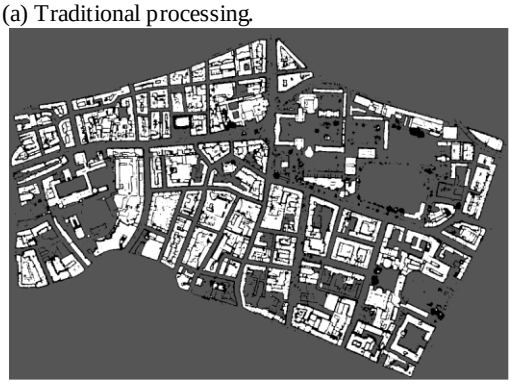
(b) Alternative processing using contour analysis.
Fig. 14. Results of automatic building identification.

Ideally, the resulting FEM meshes would be three-dimensional (3D), but to begin to achieve this, a two-dimensional (2D) approach has first been adopted. Given that much of the tunnelling community still considers building damage prediction based upon a plane-strain scenario, the creation of 2D meshes remains a reasonable short-term goal.

For this portion of the pipeline, a major innovation was achieved. Specifically a spatial index structure known as an octree was applied to the data set (Fig. 15). This allows the data to be positionally described by repeatedly subdividing the dataset into eight congruent cubic blocks (also known as voxels) up to a user-specified tiling level. There are various criteria that can be applied to determine how much subdivision occurs (Hinks et al., 2009b). As shown in Fig. 16, a data set was recursively subdivided eight times, and major structures are clearly visible.

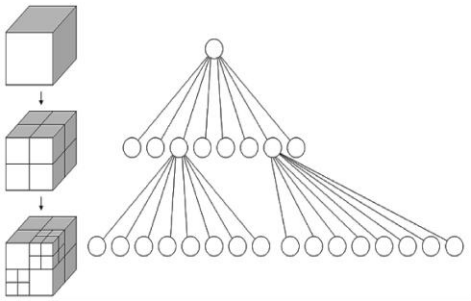

Fig. 15. Octree structure.

Fig. 16. Octree applied to LiDAR data set.

The voxelization permits a rather simple format to further manipulate into a solid model as the input file for a commercial FEM software package. The details of this are provided elsewhere (Hinks et al., 2009b).

Figure 17 depicts the transformation of the LiDAR data into a usable FEM mesh. Although the mesh is not fully reflective of the building's detailed geometry, it shows the potential of the technique. In this case, the critical breakthrough shown iss that even with the relatively sparse sampling of the aerial LiDAR data (as opposed to its terrestrial counterpart), the proposed two-step technique of octree application and voxelization can result in an FEM mesh that can be generated and can converge with no manual intervention and no a priori information. The mesh is shown stressed only under self-weight (fig. 17e). Lighter areas show those portions of the structure with higher stresses. From a qualitative perspective, the model reacts as expected by exhibiting higher stress levels in more slender members and around the window openings.

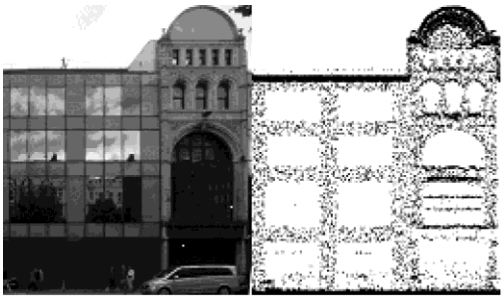

(a) Photograph. (b) LiDAR data.

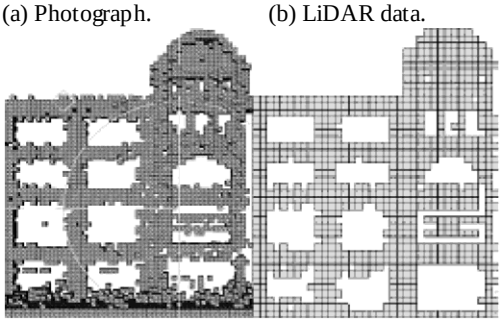

(c) Voxelization. (d) Solid Model.

(e) FEM Stress Analysis Results.

Fig. 17. Pipeline for automated data conversion from LiDAR to solid model into an FEM format (using ANSYS), with verification shown under self-weight loading.

Based on these demonstrable advances, the next steps involve the further geometric optimization and verification of these techniques. They are the main emphasis of current research efforts by the authors.

4. CONCLUSIONS

This paper presents an overview of critical new advances in the creation of a fully automated pipeline to generate accurate finite element meshes from LiDAR data. Key steps include (1) changes in flight path based data capture; (2) disaggregation and subsequent mining of latent data within each LiDAR point based on a knowledge of the structure of the data acquisition process and known location of the scanner; (3) statistically based post-process for building wall identification; (4) application of contour analysis methods to generate a fail-safe building detection process as verified through flood filling; (5) data transformation from LiDAR point clouds into FEM meshes through the application of an octree spatial index and its subsequent voxelization as verified through the stress analysis generated by simple self-weight loading. The advances herein hold strong promise for providing the underpinnings of the next generation of urban modelling.

5. ACKNOWLEDGMENTS

Support for this work was generously provided by Science Foundation Ireland, Grant 05/PICA/I830 and the Environmental Protection Agency Grant 2005-CD-U1-M1.

6. REFERENCES

Baltsavias, E.P. 1999. Airborne laser scanning - an introduction and overview. *ISPRS Journal of Photogrammetry & Remote Sensing*, Vol. 54, No. 2-3, pp. 68-82.

Forlani, G., Nardinocchi, C., Scaioni, M. & Zingaretti, P. 2006, Complete Classification of Raw LIDAR Data and 3D Reconstruction of Buildings. *Pattern Analysis Applications*, Vol. 8, pp. 357–374.

Hinks, T., Carr, H. & Laefer, D.F. 2009a. Flight Optimization Algorithms for Aerial LiDAR Capture for Urban Infrastructure Model Generation, *Journal of Computing in Civil Engineering*, Vol. 23, No. 4, pp. 330-339.

Hinks, T., Carr, H., Laefer, D.F., Morvan, Y. & O'Sullivan, C. 2009b. Robust Building Outline Extraction. PTO 56793223.

Hollaus, M., Wagner, W. & Kraus, K. 2005. Airborne laser scanning and usefulness for hydrological models. *Advances in Geosciences*, Vol. 5, pp. 57-63.

Laefer, D.F. & Pradhan, A. 2006. Evacuation Route Selection Based on Tree-Based Hazards Using LiDAR and GIS. *J. Transportation Eng.*, ASCE, Vol. 132, No. 4, pp. 312-20.

Rottensteiner, F. 2003. Automatic generation of high-quality building models from lidar data. *IEEE Computer Graphics and Applications*, Vol. 23, No. 6, pp. 42–50.

Truong-Hong, L. & Laefer, D.F. (2010, in review). Impact of Modeling Architectural Detailing for Predicting Unreinforced Masonry Subsidence Damage. *Int'l J. Arch'l Heritage*, Taylor & Francis.